ANTIOXIDANTS & REDOX SIGNALING
Volume 11, Number 9, 2009

DOI: 10.1089/ars.2009.2459

The Role of NADPH Oxidase 1–Derived Reactive Oxygen Species in Paraquat-Mediated Dopaminergic Cell Death

Ana Clara Cristóvão,[1,2,3] Dong-Hee Choi,[1] Graça Baltazar,[3] M. Flint Beal,[1] and Yoon-Seong Kim[1]

Abstract

Oxidative stress is the common downstream effect of a variety of environmental neurotoxins that are strongly implicated in the pathogenesis of Parkinson's disease. We demonstrate here that the activation of NADPH oxidase 1 (Nox1), a specialized superoxide-generating enzyme complex, plays a key role in the oxidative stress and subsequent dopaminergic cell death elicited by paraquat. Paraquat increased the expression of Nox1 in a concentration-dependent manner in rat dopaminergic N27 cells. Rac1, a key component necessary for Nox1-mediated superoxide generation, also was activated by paraquat. Paraquat-induced reactive oxygen species generation and dopaminergic cell death were significantly reduced after pretreatment with apocynin, a putative NADPH oxidase inhibitor, and Nox1 knockdown with siRNA. Male C57BL/6 mice received intraperitoneal (IP) injections of paraquat (10 mg/kg) once every 3 days and showed increased Nox1 levels in the substantia nigra as well as a 35% reduction in tyrosine hydroxylase–positive dopaminergic neurons 5 days after the last injection. Preadministration of apocynin (200 mg/kg, IP) led to a significant decrease in dopaminergic neuronal loss. Our results suggest that Nox1-generated superoxide is implicated in the oxidative stress elicited by paraquat in DA cells, and it can serve as a novel target for pharmacologic intervention. *Antioxid. Redox Signal.* 11, 2105–2118.

Introduction

ALTHOUGH the specific etiology of Parkinson's disease (PD) remains largely elusive, aging, genetic susceptibility, and exposure to environmental toxic compounds contribute to the development of PD. Based on epidemiologic studies showing that persons living in rural areas, who farm and drink well water, have a higher PD incidence, it has been widely postulated that agricultural agents may be linked to PD pathogenesis (5, 10). Paraquat (1,1′-dimethyl-4,4′-bipyridinium dichloride, PQ), a widely used herbicide, is in this category and is considered a key risk factor. Epidemiologic studies demonstrated the association between prolonged exposure to PQ and increased risk for developing PD (28, 39). Although the molecular mechanisms governing PQ toxicity to the nigrostriatal dopaminergic (DA) system are still under extensive investigation, its abilities to produce superoxide *via* the redox cycling and to induce ROS generation by mitochondrial inhibition suggest PQ as an oxidative stressor (22). Various cellular reductases can catalyze the one-electron reduction of PQ to a cation radical, which, by transferring its electron onto molecular oxygen, would readily form superoxide anion. The production of superoxide radical also regenerates a PQ parent compound (11, 22). This redox cycling has the potential to yield large amounts of reactive oxygen species (ROS) from relatively small concentrations of an agent (17, 22).

A growing body of evidence has demonstrated that oxidative stress is a key player in the pathogenesis of PD. DA neurons are extremely sensitive to insult. This selective vulnerability of the nigrostriatal system to oxidative stress is based on the following observations: (a) the generation of ROS during the oxidative metabolism of dopamine (25); (b) the capability of its quinone metabolites to adduct proteins containing a sulfhydryl group such as glutathione (6, 34); and (c) the high level of iron in the substantia nigra (SN) and globus pallidus that contributes to the highly reactive hydroxyl radical (OH^-) generation *via* the Fenton reaction (21, 26). The idea is supported by studies of postmortem brain tissues from PD patients demonstrating high oxidative stress levels in the SN, marked by increased lipid peroxidation (20), protein (2) and DNA (60) oxidative damage, and decreased

[1]Neurology/Neuroscience Department, Weill Medical College of Cornell University, New York, New York.
[2]PhD Program in Experimental Biology and Biomedicine, Center for Neuroscience and Cell Biology, University of Coimbra, Coimbra; and
[3]Health Sciences Research Center, University of Beira Interior, Covilhã, Portugal.

glutathione levels (46, 54). Mitochondrial dysfunction also has been implicated in PD pathogenesis, partly through an increase in ROS generation. Mitochondrial respiratory chain complex I activity is selectively decreased in the SN of PD postmortem brains, whereas other electron-transport complexes remain unchanged (51). Complex I inhibitors, such as 1-methyl-4-phenylpyridinium (MPP^+), the reactive product of 1-methyl-4-phenyl-1,2,3,6-tetrahydropyridine (MPTP) and rotenone, cause oxidative stress followed by DA neuronal loss that replicates the hallmarks of PD in rodents (7, 53). Inflammation mainly caused by microglial activation in the central nervous system (CNS) is also responsible for the PD pathogenesis. Superoxide and nitrogen oxide (NO) are directly secreted from activated microglia and lead to DA neuronal degeneration (24, 30).

Nicotinamide adenine dinucleotide phosphate (NADPH) oxidase was originally discovered in phagocytes (50). In these cells, the enzyme is responsible for killing bacteria through the release of substantial quantities of superoxide into the phagosomes. Although several organelles including mitochondria and biological reactions physiologically generate ROS as a by-product, the NADPH oxidase (Nox) system functions primarily as a superoxide generator. The recent discovery of several isoforms of the Nox family reveals that this specialized ROS-generation system is not limited to phagocytes (14, 18, 55). Within the CNS, studies have focused primarily on microglial $gp91^{phox}$ (Nox2). *Nox2* knockout led to reduced DA toxicity caused by PQ in both *in vitro* and *in vivo* studies (47, 59). Recent studies have shown, however, that various Nox homologues are expressed in neurons as well as in astrocytes (33).

Based on this background, we investigated whether DA cells are equipped with the NADPH oxidase system, and if this system is readily activated by toxic insults such as PQ to produce ROS, and results in DA neurodegeneration.

Materials and Methods

Materials

Fetal bovine serum (FBS), horse serum, RPMI 1640, L-glutamine, trypsin/EDTA, and penicillin–streptomycin were purchased from GibcoBRL (Gaithersburg, MD). Phenylmethylsulfonyl fluoride (PMSF), Nonidet P-40 (NP-40), SP600125, Brij35, and bupropion were purchased from Sigma Chemicals (St. Louis, MO). Rabbit polyclonal anti-tyrosine hydroxylase (TH) was obtained from Protos Biotech (New York, NY), rabbit anti-Nox1 from Santa Cruz Biotechnology (Santa Cruz, CA), and rat anti-CD11b from Serotec (Raleigh, NC). Anti-goat IgG, anti-rat IgG, and anti-rabbit IgG antibodies were from Jackson ImmunoResearch (West Grove, PA). Enhanced chemiluminescence kit was obtained from Pierce (Rockford, IL), and Taq polymerase, from Roche Applied Science (Indianapolis, IN). Vectastain ABC kit, biotinylated anti-rabbit, anti-mouse IgG, or anti-rat IgG were from Vector Laboratories (Burlingame, CA). Trizol reagent, 2′,7′-dichlorodihydrofluorescein diacetate (DCFDA), dihydroethidium (DHE), MitoSOX Red mitochondrial superoxide indicator, BLOCKiT Fluorescent Oligo, Lipofectamin, superscript II reverse transcriptase, 10–20% sodium dodecylsulfate (SDS), polyacrylamide gel, and 10–20% tricine gel were purchased from Invitrogen (Carlsbad, CA). Rac1 activation kit was purchased from Cell Biolab, Inc. (San Diego, CA). Apocynin, paraquat, 3-(4,5-dimethylthiazal-2-yl)-2,5-diphenyl-tetrazolium bromide (MTT), protease inhibitor cocktail {AEBSF, aprotinin, bestatin hydrochloride, E-64-[*N*-(*trans*-epoxysuccinyl)-L-leucine 4-guanidinobutylamide], leupeptin, pepstatin A}, nitroblue tetrazolium (NBT) and dimethylsulfoxide (DMSO) were from Sigma-Aldrich (St. Louis, MO). CytoTox-96-NonRadioactive-Cytotoxicity-Assay for LDH activity was from Promega Bioscience (San Luis Obispo, CA). All other chemicals of reagent grade were from Sigma Chemicals or Merck (Rahway, NJ).

Animals and treatment paradigm

The experiments were carried out on mice, in accordance with the NIH *Guide for the Care and Use of Laboratory Animals*. All procedures were approved by the local Animal Care and Use Committee. Male C57BL/6 mice [Charles River (Wilmington, MA); 8 to 10 weeks] were maintained in a temperature/humidity-controlled environment under a 12-h light/dark cycle with free access to food and water. As depicted in Fig. 5A and B, each animal received three IP injections, separated by 2 days, of either vehicle (1% of DMSO in saline), PQ (10 mg/kg of body weight) or PQ combined with apocynin (200 mg/kg of body weight; Apo), according to previously published dosing (27, 40).

For the group co-treated with PQ and apocynin, an injection of apocynin was given before as well as on the day of the PQ injection. Five days after the last injection, animals were killed and were intracardially perfused for immunohistochemical analysis.

A time-course study (Fig. 5B) was also performed, in which the animals were intracardially perfused for immunohistochemical analysis 1 day after the first and second PQ injection and 5 days after the last injection. In this study, for the group co-treated with apocynin and PQ, apocynin was given before as well as on the day of the PQ injection, and the animals were killed 5 days after the last PQ injection (day 12).

In total, 38 mice (vehicle, PQ, and PQ+ Apo) were used in this study.

Cell-culture and treatment paradigm

The immortalized rat mesencephalic dopaminergic cell line (N27 cells) was grown in RPMI 1640 medium containing 10% FBS, 100 units of penicillin, and 50 μg/ml streptomycin in a humidified atmosphere of 5% CO_2 at 37°C. For experiments, the cells were plated on polystyrene tissue-culture dishes at a density of 1×10^4 cells per well in 96-well culture plates, 0.5×10^5 cells per well in 24-well culture plates, 1.5×10^5 cells/well in six-well culture plates, or 5×10^5 cells per 100-mm dish. After 18 h, cells were treated with different concentrations of PQ or apocynin or both for the indicated duration. For siRNA transfection experiments, cells were plated at a density of 2×10^4 cells per well in 96-well culture plates and 5×10^5 cells per 60-mm dish.

Lactate dehydrogenase assay and MTT reduction assay

The extent of cell death was assessed by using the cytotoxic assay kit to evaluate the activity of lactate dehydrogenase (LDH) released into the culture medium. Aliquots (50 μl) of cell-culture medium were incubated at room temperature in

the presence of 0.26 m*M* NADH, 2.87 m*M* sodium pyruvate, and 100 m*M* potassium phosphate buffer (pH 7.4) in a total volume of 200 $\mu\lambda$, for 15–30 min. The levels of NAD^+ formation were measured at 490 nm by using a microplate spectrophotometer (SPECTRA MAX 340 pc; Molecular Devices, Sunnyvale, CA). To assess cell viability, levels of MTT reduction were measured. After 24-h PQ treatment, N27 cells were incubated with 0.5 mg/ml of MTT in medium overnight at 37°C. MTT is converted by viable cells to a water-insoluble precipitate that was dissolved in 10% SDS and colorimetrically quantified (O.D., 570 nm) by using a microplate spectrophotometer.

Determination of cellular ROS content

ROS levels were measured by using three different methods: DCFDA, DHE, and NBT assays. The DCFDA assay is based on the principle that the 2′,7′-dichlorodihydrofluorescein diacetate can be oxidized by ROS and converted to the fluorescent 2′,7′-dichlorofluorescein. In the DHE assay, blue fluorescent DHE can be dehydrogenated by superoxide (O_2^-) to form a red fluorescent ethidium bromide. The NBT assay is based on the conversion of NBT to NBT diformazan (formazan dye) by superoxide radicals. PQ-treated cells were incubated with DCFDA (150 μM), DHE (150 μM), and NBT (0.3 mg/ml) in complete medium for 1, 4, and 6 h at 37°C, respectively. To measure the fluorescence produced in the DCFDA and DHE, the medium was removed, and PBS was added to each well. The emitted fluorescence was read in a microplate spectrophotometer plate reader at Ex/Em 502/535 or 525/620 nm for the DCFDA or DHE assays, respectively. To quantify NBT precipitation, cells were washed twice with 70% methanol and fixed for 5 min in 100% methanol. Wells were allowed to air dry, and the water-insoluble formazan was solubilized with 120 μl 2 *M* KOH and 140 μl DMSO. The optical density was read in a microplate spectrophotometer plate reader at 590 nm.

Western blot analysis

Cells were washed with ice-cold PBS and lysed on ice in RIPA buffer (50 m*M* Tris/HCl, pH 8.0, 150 m*M* NaCl, 2 m*M* sodium orthovanadate, 1% Nonidet-P40, 0.5% sodium deoxycholate, 0.1% SDS, containing 1% of a protease inhibitor mixture (AEBSF, pepstatinA, E-64, bestatin, leupeptin, and aprotinin) purchased from Sigma-Aldrich. The soluble fraction was obtained, and equal amounts of cell lysate protein were loaded in each lane of 10–20% SDS polyacrylamide gel. After electrophoresis and transfer onto a polyvinylidene difluoride membrane, specific protein bands were detected by using appropriate primary (rabbit anti-Nox1; mouse anti-β-actin) and secondary antibodies followed by enhanced chemiluminescence.

Rac1 activation assay

To assess Rac1 activation, we used the Rac Activation Assay Kit, from Cell Biolabs, Inc. (SKU STA-401; San Diego, CA). We followed the protocol provided by the manufacturer. In brief, N27 cells were treated with 500 and 800 μM PQ for 8 h, followed by total cellular proteins extraction. Of the total cellular proteins, I mg was incubated with 10 mg of agarose beads containing the p21-binding domain (PBD) of the p21-activated protein kinase 1 (PAK1), an effector of activated Rac, for 1 h at 4°C. The beads were collected by centrifugation and washed two times in the lysis buffer. The beads were resuspended in sample buffer and boiled for 5 min. Proteins were resolved by SDS-PAGE with a 10–20% Tricine gel, transferred electrophoretically, and visualized by using anti-rat Rac1 antibody followed by enhanced chemiluminescence. For the positive control, the nonhydrolyzable GTP analogue GTPgS was used according to the manufacturer's protocol.

Preparation and transfection of siRNA

Sense and antisense oligonucleotides corresponding to the rat Nox1 cDNA sequences 5′-CCTTTGCTTCCTTCTTGAAA TCTAT-3′, which does not contain any sequences homologous to other Nox enzymes, were used. The double-stranded siRNAs were synthesized chemically and modified into stealth siRNA to enhance the stability *in vitro*. As negative control, stealth siRNA with a GC content similar to that of Nox1 stealth siRNA was used. When N27 cell cultures reached ~80% confluence in 96-well culture plates or 60-mm dishes, transfection by adding Lipofectamin 2000 and siRNAs (final concentration, 33 n*M*) was performed. After 6 hr of incubation, the culture medium was changed, and cells were maintained for additional 36 h before PQ treatment. To evaluate transfection efficiency, N27 cells were also transiently transfected with siRNA tagged with fluorescence (BLOCKiT Fluorescent Oligo) for 36 h, and transfected cells were identified by green fluorescence in cells. Double-stranded siRNAs, the negative control stealth siRNA, as well as the BLOCKiT Fluorescent Oligo, were purchased from Invitrogen.

Immunohistochemistry

After perfusion with saline and 4% paraformaldehyde in phosphate-buffered saline (PBS), brains were removed, and forebrain and midbrain blocks were immersion-fixed in 4% paraformaldehyde and cryoprotected in sucrose. Serial coronal sections (40 μm) were cut on a cryostat, collected in cryopreservative, and stored at −20°C. For immunolabeling studies, sections were incubated with blocking solution (5% horse serum and 0.3% Triton X-100 in PBS, pH 7.5) and then with primary antibodies at room temperature overnight. Finally, sections were incubated with secondary antibodies in blocking solution at room temperature for 1 h. The primary antibodies used were rabbit anti-TH antibody (1:10,000; Protos Biotech, New York, NY), rabbit anti-Nox1 (1:500; Santa Cruz Biotechnology, rat anti-CD11b (1:50; Serotec, Raleigh, NC). The secondary antibodies were biotinylated anti-rabbit IgG or anti-rat IgG (1:200; Vector Laboratory and following the staining procedure outlined by the manufacturer of the Vectastain ABC kit in combination with 3,3′-diaminobenzidine reagents. The same TH-stained sections were then counterstained with Nissl (0.25% cresyl violet) for 5 min, washed in distilled water, air dried, cleaned in xylene, and then mounted with the appropriate mounting medium. The numbers of TH-immunoreactive cells and Nissl-positive cells in the SN pars compacta (SNpc) were counted by using an optical fractionator. Analysis was performed by using a system consisting of a Nikon Eclipse E600 microscope (Morrell Instruments Co. Inc., Melville, NY) equipped with a computer-controlled

LEP BioPoint motorized stage (Ludl Electronic Products, Hawthorne, NY), a DEI-750 video camera (Meyer Instruments, Houston, TX), a Dell Dimension 4300 computer (Dell, Round Rock, TX), and the Stereo Investigator (v. 4.35) software program (Microbrightfield, Burlington, VT). Tissue sections were examined by using a Nikon Plan Apo 100x objective lens with a 1.4 numeric aperture. The size of the x–y sampling grid was 140 μm. The counting-frame thickness was 14 μm, and the counting-frame area was 4,900 μm^2.

Total RNA extraction and RT-PCR analysis

Total RNA was extracted from N27 cells by using Trizol reagent. Reverse transcription (RT) was performed for 40 min at 42°C with 1 μg of total RNA by using 1 unit/$\mu\lambda$ of superscript II reverse transcriptase. Oligo (dT) and random primers were used as primers. The samples were then heated at 94°C for 5 min to terminate the reaction. The cDNA obtained from 1 μg total RNA was used as a template for PCR amplification. Oligonucleotide primers were designed based on Genebank entries for rat Nox1 (sense, 5′-TGACAGTGATGTATGCAG CAT-3′; antisense, 5′-CAGCTTGTTGTGTGCACGCTG-3′), rat Nox2 (sense, 5′-ACTCGAAAACTTCTTGGGTCAG-3′; antisense, 5′-TCCTGTGATGCCAGCCAACCGAG-3′), rat Nox3 (sense, 5′-GCTGGATTTTGAACGAGAGTGTG-3′; antisense, 5′-GCCAGAGAGATCACCAGGCCAGT-3′), rat Nox4 (sense, 5′-GCCGGCGGTATGGCGCTGTC-3′; antisense, 5′-CCACC ATGCAGACACCTGTCAGG-3′), and rat GAPDH (sense, 5′-ATCACCATCTTCCAGGAGCG-3′; antisense, 5′-GATGGCA TGGACTGTGGTCA-3′). PCR mixes contained 10 μl of 2x PCR buffer, 1.25 m*M* of each dNTP, 10 pmol each of forward and reverse primers, and 2.5 units of Taq polymerase to a final volume of 20 μl. For Nox1, amplification was performed in 32 cycles for 40 s at 95°C, 30 s at 62°C, and 2 min at 72°C, and for Nox2, Nox3, and Nox4, it was performed in 27 cycles for 40 s at 95°C, 30 s at 58°C, and 2 min at 72°C. After the last cycle, all samples were incubated for an additional 7 min at 72°C. PCR fragments were analyzed on 1% agarose gel containing ethidium bromide, and their amounts were normalized against amplified GAPDH. Each primer set specifically recognized only the gene of interest, as indicated by amplification of a single band of the expected size.

Data analysis and statistics

Data are expressed as percentages of values obtained in control conditions and are presented as mean ± SEM of at least three experiments, in independent cell cultures. Statistical analysis was performed by using a one-way ANOVA followed by the Dunnett test or the Bonferroni Multiple Comparison Test. Values of $p < 0.05$ were considered significant.

Results

Paraquat-mediated ROS generation and subsequent dopaminergic cell death

It is known that PQ directly generates superoxide through redox cycling. To evaluate the effect of this compound on ROS generation, we treated N27 cells with various concentrations of PQ (100, 500, 800, or 1,000 μM) for 24 h and measured ROS levels with NBT, DCFDA, and DHE assays. The results obtained by using the NBT assay showed that cultures treated with 100 μM PQ showed 34 ± 2.3% higher levels of ROS than did control cultures. The levels of ROS were further increased in cultures treated with higher concentrations of PQ: 70 ± 4.5% increase in cultures treated with 500 μM, 65 ± 4.6% increases with 800 μM, and 111 ± 7.2% increase with 1,000 μM of PQ (Fig. 1A). When ROS was measured with DCFDA (Fig. 1B), similar changes were observed (46 ± 13%, 53 ± 7%, and 82 ± 11% increase in 500, 800, and 1,000 μM PQ, respectively),

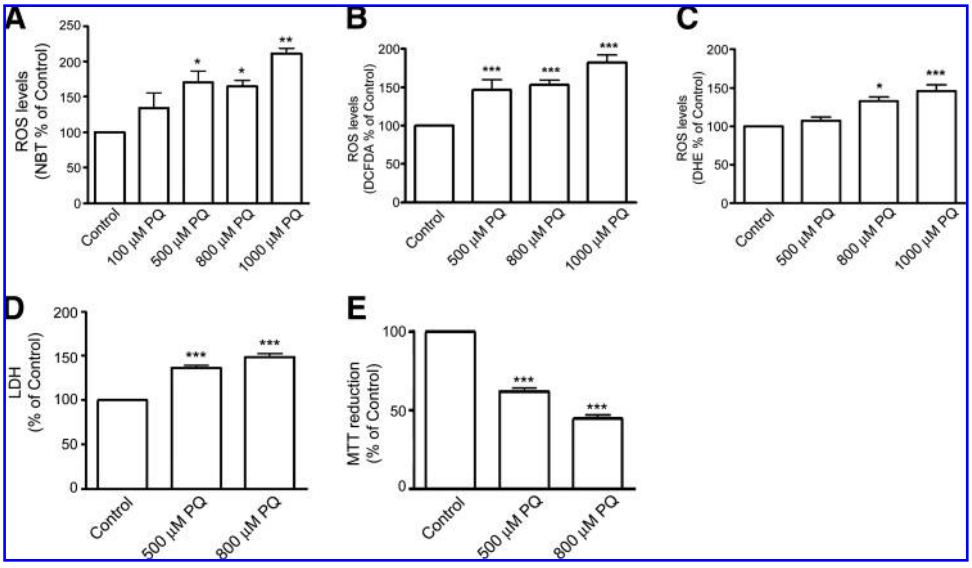

FIG. 1. PQ-mediated ROS generation and N27 DA cell death in a concentration-dependent manner. (**A**) ROS levels in N27 cells treated with PQ (100, 500, 800, or 1,000 μM) for 24 h was measured by using the NBT assay (**A**). ROS levels in N27 cells treated with PQ (500, 800 or 1,000 μM) for 24 h measured by using DCFDA (**B**) or DHE (**C**). (**D, E**) Cell-death extent was accessed by measuring the levels of LDH activity (**D**) and MTT reduction (**E**) in N27 cultures incubated with 500 or 800 μM PQ for 24 h. The results are expressed as percentage of control. Data are shown as the mean ± SEM of three independent experiments performed in triplicate. Statistical analysis was performed by using one-way ANOVA followed by Bonferroni's Multiple Comparison Test. *$p < 0.05$, **$p < 0.01$, and ***$p < 0.001$ *versus* control cultures.

whereas the DHE assay (Fig. 1C) showed that significant superoxide increase was elicited only by 800 and 1,000 μM PQ ($33 \pm 5\%$ and $45 \pm 7\%$ increase compared with control, respectively). To evaluate the effect of PQ on DA cell death, we investigated the levels of LDH and reduced MTT in N27 cells after treatment with 500 or 800 μM PQ for 24 h. As depicted in Fig. 1D, LDH levels were increased by $36 \pm 4\%$ in cultures treated with 500 μM PQ and increased by $49 \pm 6\%$ in cultures treated with 800 μM, in comparison with control cultures. Similar results were obtained in MTT assays measuring viable cells that are capable of reducing MTT. Cultures treated with 500 μM PQ showed $62 \pm 1.4\%$ of the cell viability, and only $44 \pm 2.8\%$ cells survived in cultures treated with 800 μM PQ (Fig. 1E). As demonstrated in a previous study (45), these results showed that PQ elevates ROS levels in N27 cells and finally leads to DA cell death in a concentration-dependent manner.

Paraquat-mediated increase in Nox1 expression and the activation of Rac1 in dopaminergic cells

The Nox system catalyzes the reduction of molecular oxygen and oxidation of NADPH to generate superoxide radicals and, in this way, contributes to PQ redox cycling and eventually to its toxicity. We investigated whether DA cells have the NADPH oxidase enzyme complex and whether it is affected by PQ. We evaluated mRNA levels of Nox1 in N27 DA cells treated with 500 or 800 μM PQ for 6 h, as well as in nontreated controls. Interestingly, we observed that mRNA levels of Nox1, the first Nox2 homologue identified in nonphagocytic cells, were significantly increased by PQ in a concentration-dependent manner (Fig. 2A, upper panel). N27 cells had all components of Nox1 activation, including Rac1, Noxa1, and Noxo1 (data not shown). Cultures treated with 500 μM PQ showed a $163 \pm 13\%$ increase in Nox1 mRNA

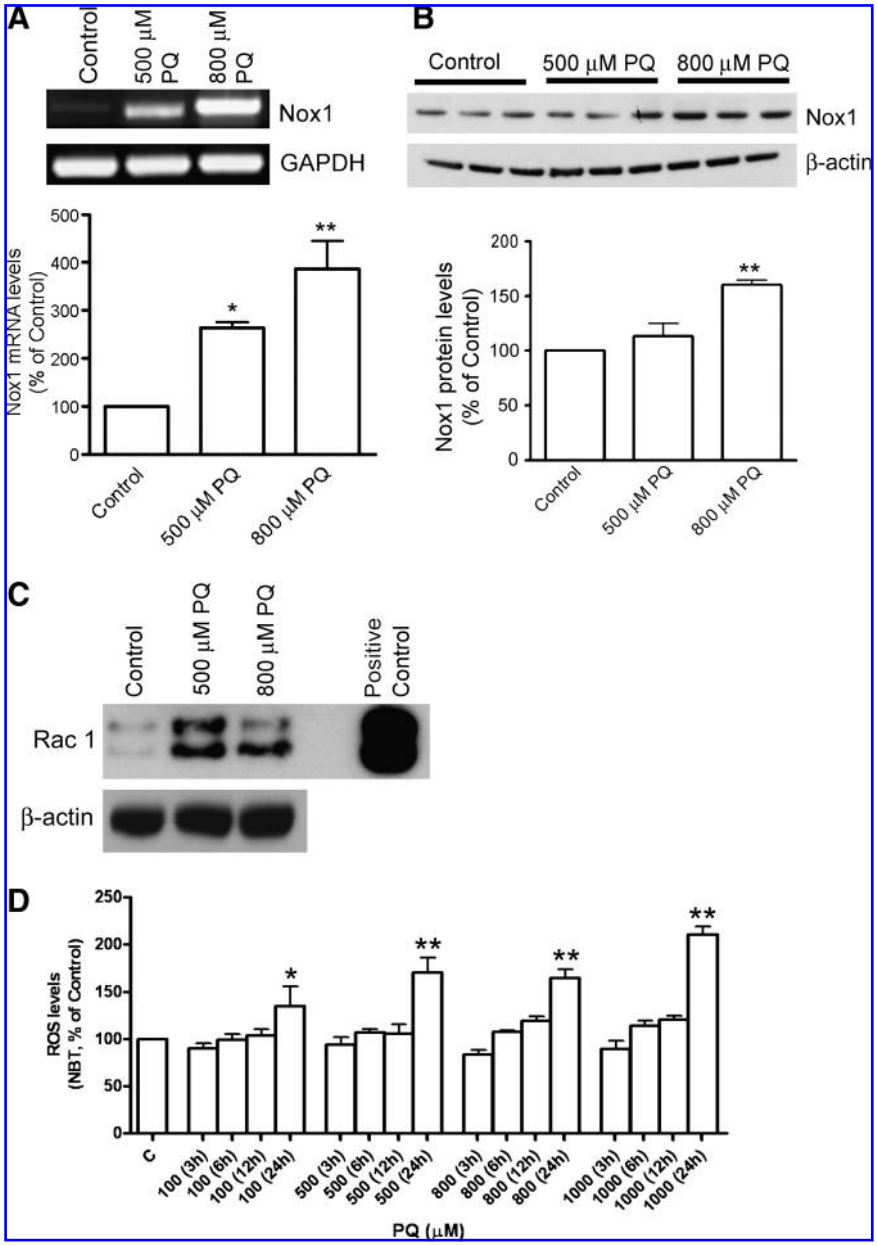

FIG. 2. Increased Nox1 expression levels and the activation of Rac1 in N27 DA cells treated with PQ. (**A**) Nox1 mRNA level was detected with RT-PCR (*upper panel*), in N27 cells treated with 500 or 800 μM PQ for 6 h, and quantified with Quantity One software and then normalized to GAPDH, an internal control (*lower panel*). (**B**) Nox1 protein levels were obtained with immunoblot analysis in N27 cells treated with 500 or 800 μM PQ for 16 h (*upper panel*) and quantified by using Quantity One software (*lower panel*). β-Actin levels were measured as an internal control. (**C**) The activated fraction of Rac1 was determined in N27 cells treated with 500 or 800 μM PQ for 8 h with the active GTPase pull-down assay. β-Actin levels were measured as an internal control. (**D**) The time-course measurement of PQ-mediated ROS generation in N27 cells. ROS levels in N27 cells treated with PQ (100, 500, 800 or 1,000 μM) for 3, 6, 12 and 24 h were measured by using the NBT assay. The results are expressed as percentage of control. Data are shown as the mean $\pm$ SEM of three independent experiments. Statistical analysis was performed by using one-way ANOVA followed by Bonferroni's Multiple Comparison Test for Nox1 mRNA levels and by Dunnett's Multiple Comparison Test for Nox1 protein levels. $^{*}p < 0.05$; $^{**}p < 0.01$ *versus* control cultures.

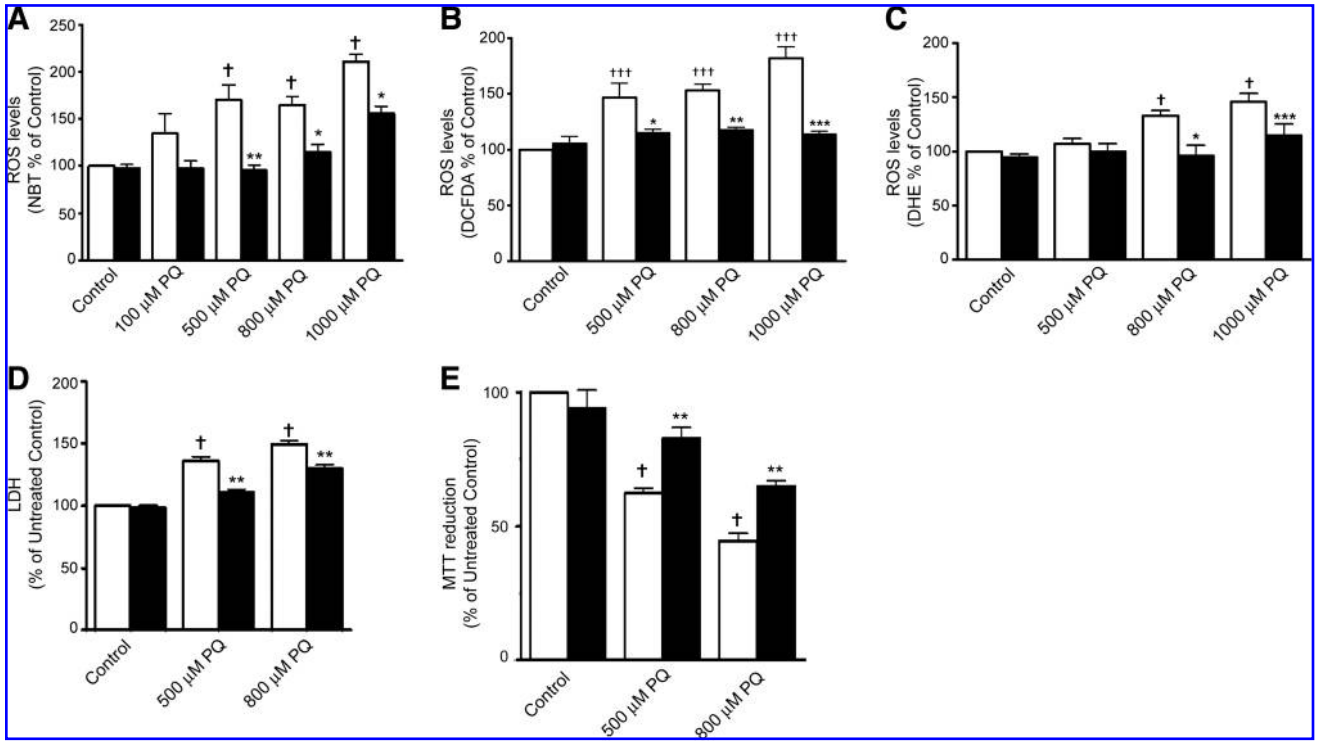

FIG. 3. Decreases in PQ-mediated ROS levels and N27 DA cell death by a putative NADPH oxidase inhibitor, apocynin (**A–C**). Apocynin significantly reduced PQ-mediated ROS generation by N27 cells. ROS levels were measured by using the NBT (**A**) assay, DCFDA (**B**), or DHE (**C**) in N27 cells pretreated with 5 μM apocynin for 1 h and then treated with various concentrations of PQ (100, 500, 800, or 1,000 μM) for 24 h. (**D, E**) Apocynin significantly reduced PQ-mediated N27 cell death. Cell-death levels were assessed by measuring the LDH activity (**D**) and MTT reduction (**E**) in N27 cultures pretreated with 5 μM apocynin for 1 h and then treated with 500 or 800 μM PQ for 24 h. The results are expressed as percentage of their controls. Data are shown as the mean ± SEM of three independent experiments performed in triplicate. Statistical analysis was performed by using one-way ANOVA followed by Bonferroni's Multiple Comparison Test. $^{*}p < 0.05$; $^{**}p < 0.01$; and $^{***}p < 0.001$ *versus* cultures pretreated with apocynin and then with PQ. $^{\dagger}p < 0.05$, and $^{\dagger\dagger\dagger}p < 0.001$ *versus* control cultures. *Solid bars*, cells pretreated with apocynin; *open bars*, cells without apocynin treatment.

levels compared with control cultures, and higher PQ doses (800 μM) increased Nox1 mRNA levels to 287 ± 62%, compared with controls (Fig. 2A, lower panel). Next, we evaluated Nox1 protein levels in N27 cells incubated for 16–18 h with or without PQ. Only cultures treated with 800 μM PQ showed a significant increase in Nox1 protein levels (60 ± 6%; Fig. 2B). Although 500 μM PQ was able to increase Nox1 mRNA (Fig. 2A), this concentration was not sufficient to increase significantly Nox1 protein levels (13 ± 10%) compared with controls (Fig. 2B). The functional activation of Nox1 is dependent on the activation of a small GTPase, Rac1 (9).

Based on these facts, we tested whether PQ induces the activation of Rac1. Activated Rac1 was limited in nontreated N27 cells. After treatment of cells with PQ for 8 h, a significant

FIG. 4. Decreases in PQ-mediated ROS levels and N27 DA cell death by Nox1 knockdown. (**A**) Transfection efficiency of Nox1 siRNA into N27 cells. (**A**) N27 cells were transiently transfected with siRNA tagged with fluorescence for 36 h. Transfected cells were identified with green fluorescence in cells, and total cells were identified with DAPI staining. Transfection efficiency was calculated as percentage of green fluorescence–positive cells to total cells stained for DAPI. Nox1 siRNA-mediated knockdown efficiency was also verified by using RT-PCR for Nox1, Nox2, Nox3, and Nox4 (**B** and **C**) and immunoblot analysis for Nox1 (**D**). N27 cells were transiently transfected with rat Nox1 siRNA, control siRNA (ctr siRNA), or exposed only to lipofectamine (non-tx) for 36 h and then treated with 1,000 μM PQ. GAPDH and β-actin were used as internal controls for RT-PCR and immunoblot, respectively. Nox1 mRNA (**C**) and protein (**D**) levels were quantified by using Quantity One software from Bio-rad. For **C** and **D**, $^{**}p < 0.01$ *versus* non-tx and $^{\dagger}p < 0.05$ *versus* ctr siRNA+PQ or *versus* non-tx+PQ or both. (**E–G**) Nox1 knockdown significantly reduced PQ-mediated ROS levels as well as N27 cell death. ROS levels were measured by using DCFDA (**E**) or DHE (**F**), and cell death was evaluated by using the LDH assay (**G**) in N27 cells transiently transfected with rat Nox1 siRNA and then treated with various concentrations of PQ (800, 1,000, 1,500, or 2,000 μM) for 24 h. $^{*}p < 0.05$; $^{**}p < 0.01$; and $^{***}p < 0.001$ *versus* control. $^{\dagger}p < 0.01$ and $^{\dagger\dagger}p < 0.05$ *versus* ctr siRNA+PQ. *Solid bars*, cells transfected with Nox1 siRNA; *open bars*, cells transfected with ctr siRNA. Data are shown as the mean ± SEM of three independent experiments performed in triplicate. Statistical analysis was performed by using one-way ANOVA followed by Bonferroni's Multiple Comparison Test.

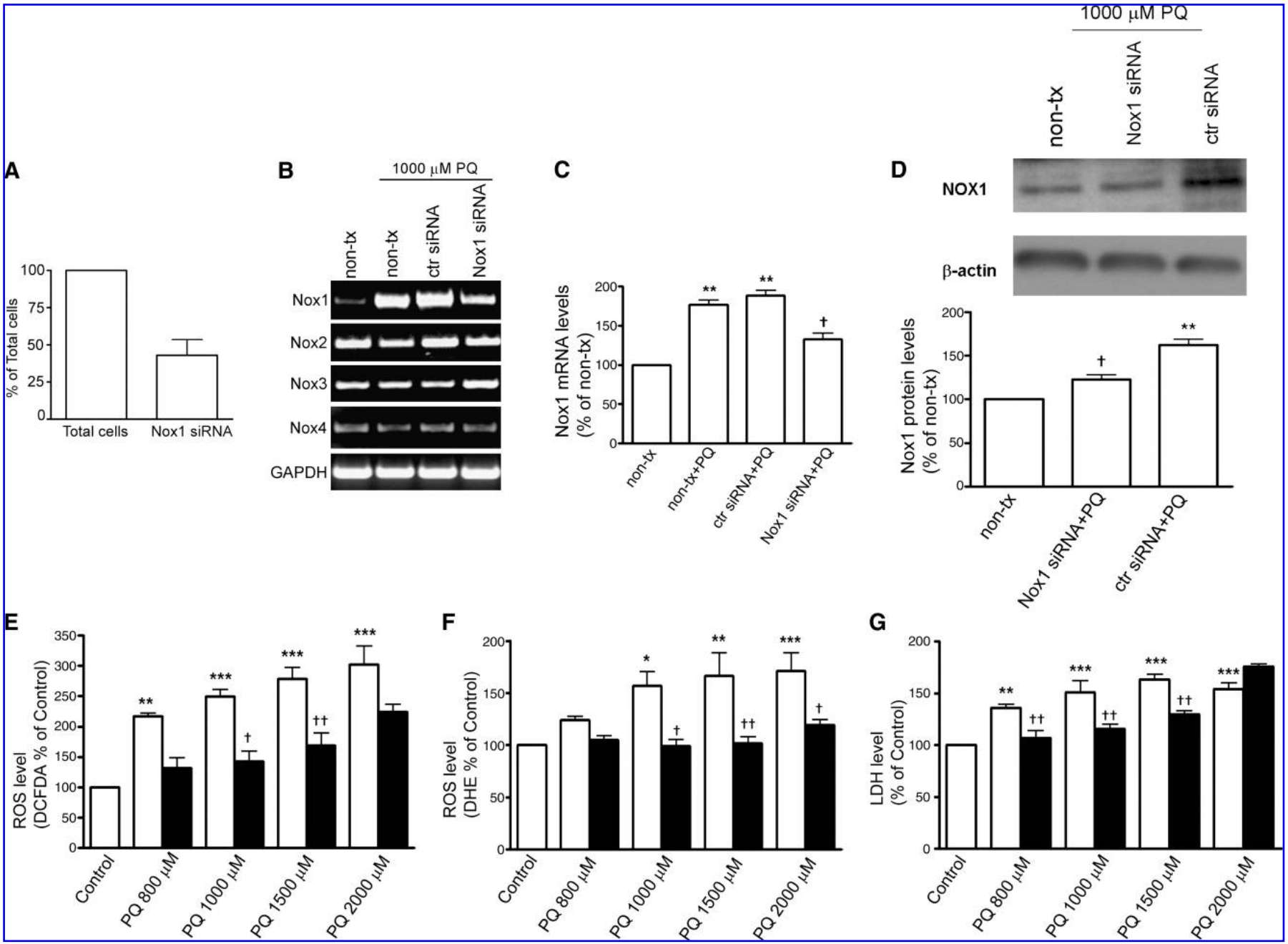
A
% of Total cells
100
75
50
25
0
Total cells
Nox1 siRNA
B
1000 μM PQ
non-tx
non-tx
ctr siRNA
Nox1 siRNA
Nox1
Nox2
Nox3
Nox4
GAPDH
C
Nox1 mRNA levels
(% of non-tx)
200
150
100
50
0
**
**
†
non-tx
non-tx+PQ
ctr siRNA+PQ
Nox1 siRNA+PQ
D
1000 μM PQ
non-tx
Nox1 siRNA
ctr siRNA
NOX1
β-actin
Nox1 protein levels
(% of non-tx)
200
150
100
50
0
†
**
non-tx
Nox1 siRNA+PQ
ctr siRNA+PQ
E
ROS level
(DCFDA % of Control)
350
300
250
200
150
100
50
0
**
***
†
***
††
***
Control
PQ 800 μM
PQ 1000 μM
PQ 1500 μM
PQ 2000 μM
F
ROS level
(DHE % of Control)
200
150
100
50
0
*
†
**
††
***
†
Control
PQ 800 μM
PQ 1000 μM
PQ 1500 μM
PQ 2000 μM
G
LDH level
(% of Control)
200
150
100
50
0
**
††
***
††
***
††
***
Control
PQ 800 μM
PQ 1000 μM
PQ 1500 μM
PQ 2000 μM

increase in activated Rac1 was observed (Fig. 2C). To investigate a sequential relation between Nox1 activation and PQ-mediated ROS generation, the time-course of ROS generation was investigated in N27 cells treated with various doses of PQ (Fig. 2D). ROS levels were significantly increased only after 24-h PQ treatment, suggesting that Nox1 activation can be responsible for PQ-mediated ROS generation.

Attenuation of PQ-mediated ROS generation and dopaminergic cell death by inhibition of NADPH oxidase

Apocynin is a putative inhibitor of NADPH oxidase activity. To clarify the specific role of NADPH oxidase in PQ-mediated ROS generation and DA cell death, we tested the effect of apocynin in N27 cells treated with PQ. N27 cells were pretreated with 5 μM apocynin for 1 h, and then different concentrations of PQ (100, 500, 800, or 1,000 μM) were added. ROS levels were measured at 24 h after PQ by using an NBT assay. Apocynin significantly reduced PQ-mediated ROS generation in N27 cells (Fig. 3A). ROS levels in cells treated with 500 and 800 μM PQ were significantly reduced compared with control levels. Apocynin was also able to significantly reduce ROS levels induced by relatively high dose of PQ (1,000 μM) by $55 \pm 5\%$. ROS levels measured by using DCFDA (Fig. 3B) or DHE (Fig. 3C) showed similar changes observed by using the NBT assay. The effect of apocynin on PQ-mediated DA cell death was also tested. Cultures were pretreated with 5 μM apocynin for 1 h and then treated with 500 or 800 μM PQ. The viability of cells was determined with LDH and MTT assays (Fig. 3D and E). Apocynin significantly reduced LDH levels by $26 \pm 7\%$ and $19 \pm 5\%$ in cultures treated with 500 μM and 800 μM PQ, respectively, compared with cultures treated with PQ alone (Fig. 3D). The levels of reduced MTT were statistically higher in cultures pretreated with apocynin than in those treated with PQ only. As shown in Fig. 3E, apocynin increased the levels of reduced MTT by $21 \pm 5\%$ and $20 \pm 4\%$ in cultures treated with 500 μM and 800 μM PQ, respectively.

Even though apocynin has been widely used in several studies as an inhibitor of the NADPH oxidase system (8, 27), recent studies also suggest that this compound may work as a direct antioxidant (3, 29). Thus, to investigate the specific role of Nox1 in PQ-mediated oxidative stress and DA cell death, siRNA-mediated Nox1 knockdown was used as an alternative tool. Transfection efficiency of siRNA nucleotide sequence into N27 cells was evaluated by using fluorescent-tagged siRNA: $42 \pm 10\%$ of total cells were efficiently transfected after 36-h incubation (Fig. 4A). Accordingly, PQ-induced mRNA (Fig. 4B and C) levels of Nox1 were significantly reduced compared with nontranfected ($43 \pm 6\%$ less) and control siRNA transfected cells ($55 \pm 5\%$ less). PQ-induced protein (Fig. 4D) levels of Nox1 were also significantly reduced ($38 \pm 7\%$) compared with cells transfected with control siRNA. To ensure selective knockdown of Nox1 by siRNA, mRNA levels of other Nox isoforms, including Nox2, Nox3 and Nox4, were determined as well. No changes were found between nontransfected cells and cells transfected with control siRNA or Nox1 siRNA (Fig. 4C). Finally, PQ-mediated ROS generation was also significantly decreased in cells transfected with Nox1 siRNA (Fig. 4E and F). PQ-mediated DA cell death was also significantly reduced by Nox1 knockdown (Fig. 4G). Although Nox1 knockdown significantly inhibited ROS generation by 2,000 μM PQ, cell death was not prevented at this concentration, implying that PQ induces cell death through pathways distinct from ROS-mediated pathways.

These results highlight that the NADPH oxidase system, and specially Nox1, plays a crucial role in PQ-mediated ROS generation as well as subsequent DA cell death.

Increased expression of Nox1 in the SN of mice treated with PQ intraperitoneally

Previous *in vivo* studies tested various PQ-injection paradigms in mice and demonstrated a selective DA neuronal death (41, 42, 49). An approximate 25% DA cell loss was reported in mice treated with 10 mg/kg IP of PQ every week for 3 weeks (42). To ensure significant levels of PQ toxicity on DA neurons, we tested a different injection paradigm, depicted in Fig. 5A. Each animal received three IP injections, separated by 2 days of either vehicle (1% of DMSO in saline), PQ (10 mg/kg), or PQ combined with apocynin (200 mg/kg). Apocynin was also administered IP 1 day before and on the same day as PQ injection. A similar dose of apocynin (300 mg/kg supplied by drinking water) showed substantially increased animal life span in ALS mice with mutant SOD1 (G93A) (27). All groups were killed 5 days after the last injection. This injection protocol resulted in about a $35 \pm 8\%$ reduction of TH-positive neurons in the SNpc compared with that in animals treated with vehicle (Fig. 7A and B). In comparison with animals treated with vehicle, those treated with PQ showed a slight decrease in body weight and overall activity. After the last injection, animals gradually recovered over the last 5 days of the experiment (data not shown). Mice treated with PQ and apocynin were more active and lost less weight, when compared with mice treated with PQ only.

We also tested another injection paradigm in which mice were treated with three injections of a higher dose of PQ (15 mg/kg) separated by 1-day intervals. At this high-dose and high-frequency paradigm, all animals died after the second injection, suggesting its systemic toxicity. These results indicate that PQ has a narrow window in which selective DA neuronal death is observed without producing overt systemic toxicity.

To verify our *in vitro* finding showing increased Nox1 levels in DA cells insulted by PQ, Nox1 levels in the SN of mice treated with vehicle or PQ were investigated with Western blot and RT-PCR analysis. As shown in Fig. 6, animals treated with PQ showed statistically higher levels of the Nox1 protein than did the animals treated with vehicle (Fig. 6A and B). Nox1 mRNA was also increased (Fig. 6C). Upregulation of Nox1 in the SN of mice injected with PQ was confirmed by immunostaining (Fig. 6D).

Apocynin reduced DA neuronal death induced by PQ in mice

Each group of animals was injected as described earlier, and the numbers of TH-positive cells and Nissl-positive cells in the SNpc were stereologically counted. As shown in Fig. 7, PQ administration led to a $35 \pm 13.7\%$ reduction of TH-

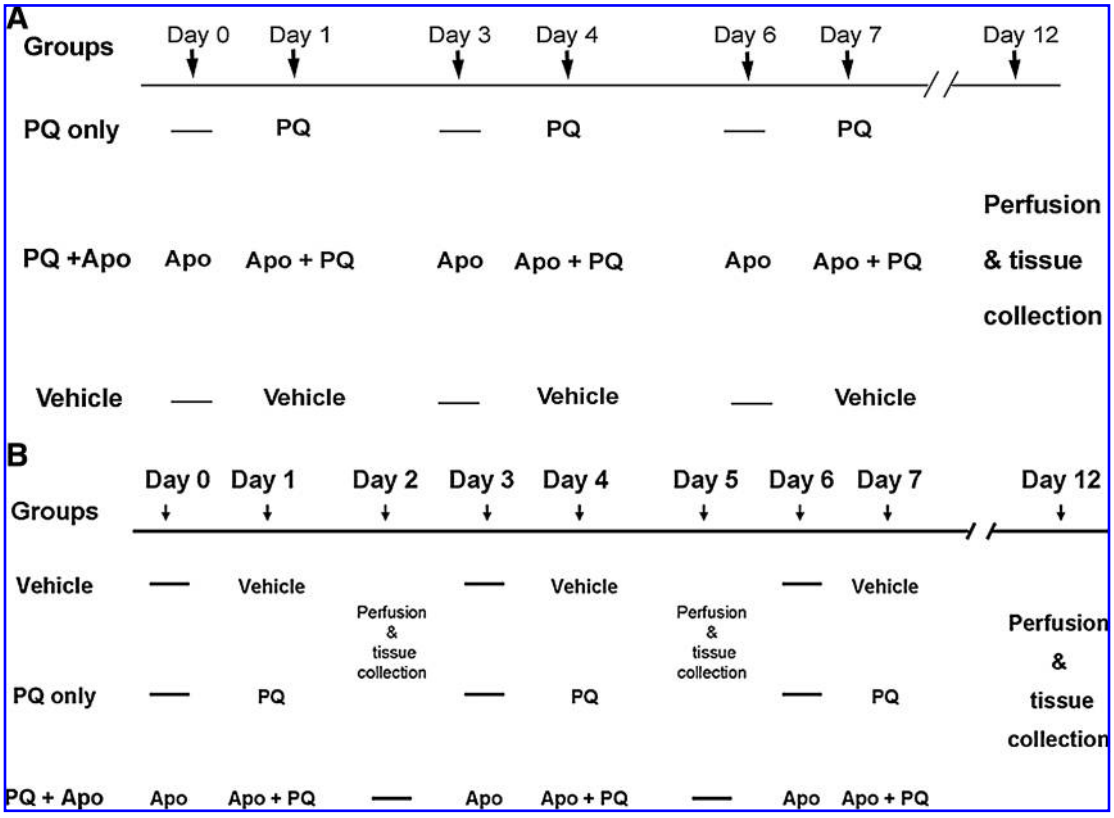

FIG. 5. PQ-injection paradigm diagram. Mice were divided into three groups. Animals were given a total of three injections of either vehicle (1% DMSO in saline), PQ (10 mg/kg of body weight), or PQ combined with apocynin (200 mg/kg of body weight) every third day. Apocynin was also administered IP 1 day before and on the same day as PQ injection. All groups were killed 5 days after the last injection (**A**); to investigate PQ-mediated microglia changes, animals were killed the day after the first and second injections and 5 days after the last injection (**B**).

positive neurons in the SNpc compared with those in animals treated with vehicle (Fig. 7A and B). Apocynin administration significantly reduced PQ-elicited TH^+ neuronal loss to $15.7 \pm 3.8\%$. Total neuronal number in the SN by Nissl staining also indicated decreased neuronal staining in the SNpc of PQ-treated mice ($25.3 \pm 6.5\%$) and that the combined treatment with apocynin elevated neuronal numbers in the SNpc to $91.3 \pm 7.8\%$ (Fig. 7A and C).

Our results support the idea that the NADPH oxidase system plays an important role in PQ-mediated DA neurotoxicity.

Paraquat-mediated microglial changes

It was previously reported that PQ exerts its toxic effects on DA neurons through microglial activation (43, 47, 59). Thus, the time-course morphologic changes in microglia in the SN after PQ treatment (Fig. 5B) were investigated with CD11b immunostaining at days 2, 5, and 12 after the first PQ injection (Fig. 8). Whereas vehicle-treated animals showed the typical ramified morphology of resting microglia, PQ treatment resulted in dramatic morphologic changes in microglia, characterized by enlarged cell bodies and loss of processes. These morphologic changes occurred at an early time point (2 days). The total number of CD11b-positive microglia was gradually decreased thereafter and was not detected at day 12 (Fig. 8A and B). Similar changes were observed in animals treated with apocynin in combination with PQ (Fig. 8A).

Discussion

In this study, we showed that the Nox complex mediates oxidative stress and cell death caused by paraquat in N27 dopaminergic cells. We identified for the first time that the Nox1 isoform is constitutively expressed in DA cells, and its level is elevated by paraquat administration both *in vivo* and *in vitro*. NADPH oxidase–derived superoxide generation and bacterial killing were first discovered in polymorphonuclear neutrophils (Nox2 or $gp91^{phox}$) (50). Nox1 is the first homologue of Nox2 that was identified in nonphagocytic cell types, including colon, prostate, uterus, and vascular smooth muscles (55). Since its discovery, a family of homologues has been identified in a variety of cells and tissues. Previous studies have shown that Nox isoforms are expressed in mouse and rat brain tissues (36, 52). In the CNS, although NADPH oxidase–mediated ROS are required for normal cellular functions, such as long-term potentiation (57) and cardiovascular homeostasis (48), excess ROS generation may contribute to pathologic conditions. Oxidative stress elicited by Nox2 in microglia, an immune component in the brain, has been widely studied in a number of brain diseases (16, 37). Recent studies, however, indicate that Nox2 expression is not limited to microglia (1),

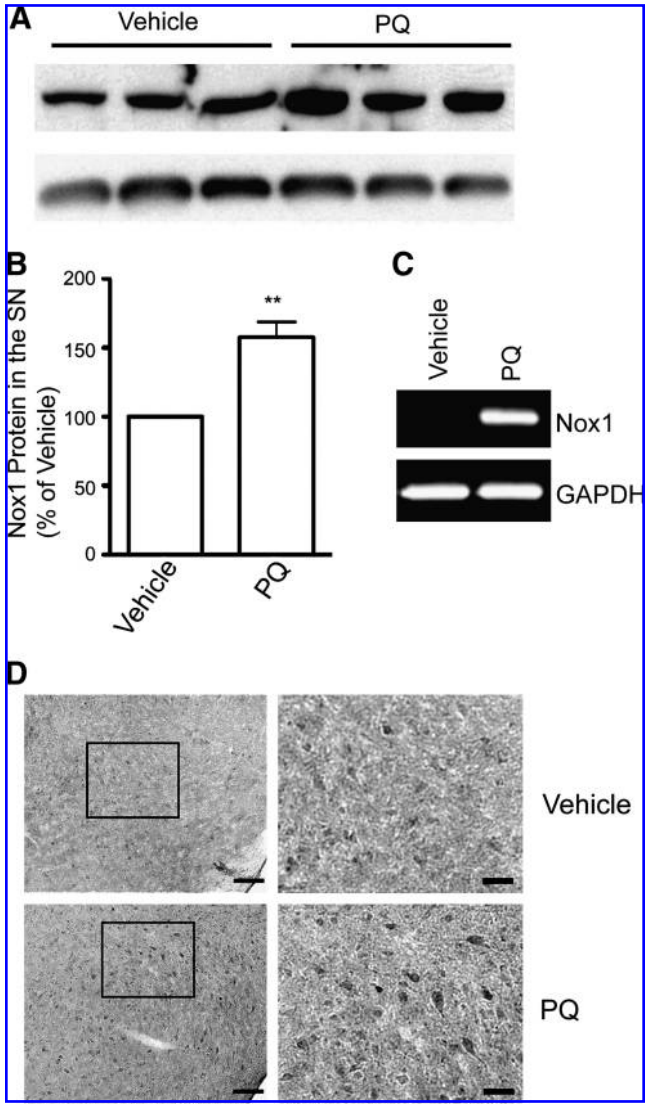

FIG. 6. Significant increase in Nox1 protein levels in the SNpc of mice injected with PQ. (**A**) Nox1 protein levels were determined in total lysates of the SN tissues of mice injected with PQ or vehicle with immunoblot analysis and RT-PCR. β-Actin and GAPDH were detected as internal control. PQ significantly increased Nox1 protein (**A, B**) and mRNA levels (**C**). Nox1 protein levels were quantified by using Quantity One software and normalized against β-actin (**B**). The results are expressed as percentage of vehicle. Data are shown as the mean $\pm$ SEM of three independent experiments ($n = 3$). Statistical analysis was performed by using one-way ANOVA followed by Bonferroni's Multiple Comparison Test. $^{**}p < 0.01$ *versus* mice treated with vehicle. (**D**) Representative photomicrograph of Nox1-immunoreactivity in the SNpc sections of mice injected with vehicle or PQ. Nox1 immunoreactivity in the SN was increased in PQ-injected animals compared with vehicle. Right panels of **D** show higher magnification of respective boxed areas in the left panels. Scale bar in the left panels = 100 μm, and in the right panels, 50 μm.

and other homologues, including Nox1, are involved in various pathologic conditions in neuronal cells. Glutamate toxicity in SH-SY5Y neuroblastoma cells is largely attenuated by inhibition of NADPH oxidase activation (44). ROS generation and apoptosis of N27 DA cells treated with MPP^+, an active metabolite of MPTP, was decreased by Nox inhibition in one study (4). In the study, however, the authors did not clearly demonstrate which isoforms are responsible for MPP^+-mediated ROS generation.

Our results demonstrated that MPP^+ increased Nox1 expression in N27 cells (data not shown), suggesting that Nox1-mediated oxidative stress might be a common feature observed in DA cells under toxic stimuli. An increasing number of studies revealed that Nox1 plays a variety of roles in various neuronal cells. Nox1-derived superoxide negatively affects NGF-mediated neurite outgrowth in PC12 cells (31). In dorsal root ganglion cells, ROS generated from Nox1 are involved in enhancing sensitivity to painful stimuli (32). Increased transcription activity of Nox1 was observed in N27 cells treated with PQ in a concentration-dependent manner. Interestingly, several studies suggested that a crosstalk between mitochondria and Nox1 induction may exist. In 293 cells, mitochondrial ROS generated under serum deprivation induces Nox1 expression and superoxide generation. Although mitochondria contribute to the early accumulation of ROS (0–4 h), the maintenance of ROS level requires PI3K/Rac1/Nox1 activation. This later phase of ROS generation and sustained accumulation by Nox1 is responsible for cell death (38). These results suggest that although the initial stage of ROS generation is responsible for triggering the Nox system, sustained superoxide production from this system is an essential component of ROS-induced cell death.

Studies of osteosarcoma cells that lack a mitochondrial genome (ρ^0) revealed that the inactivation of mitochondrial genes leads to the downregulation of Nox1 and that transfer of wild-type mitochondrial genes can restore Nox1 expression (19). Our results also confirmed that mitochondrial respiratory-chain inhibitors (including rotenone, pyridaben, antimycin A, and FCCP) elevated both mRNA and protein levels of Nox1 (data not shown). Several molecular pathways have been suggested to understand PQ-mediated oxidative stress. Despite its structural similarity with MPP^+, each compound has distinct molecular mechanisms for exerting oxidative stress and cellular damage (49). PQ is capable of directly generating superoxide through redox cycling (11), by which it may accept electrons from NAD(P)H and subsequently reduce molecular oxygen to superoxide. Mitochondrial respiratory complexes I and III both serve as targets for PQ-mediated ROS generation, with complex III showing a higher sensitivity (12, 49). Taken together, PQ-induced increase in Nox1 transcriptional activity might result from initial ROS produced by the PQ redox cycle or mitochondria. PQ may also activate signaling pathways such as PKC delta or MAPK, which were reported as Nox1 transcriptional activators (13, 23).

Nox1-mediated superoxide generation requires other components, including Rac1 activation, Noxo1 and Noxa1, and homologues of $p47^{phox}$ and $p67^{phox}$, respectively (15). Noxo1 and Noxa1 mRNAs were constitutively expressed at high levels (data not shown). Rac1, a small Rho family GTPase, is an important subunit for the activation of Nox1-derived superoxide generation (15, 58). To activate the NADPH oxidase system, activated Rac1 forms a Nox1 enzyme complex in conjunction with Noxo1 and Noxa1. In the present study, PQ-mediated Rac1 activation was observed.

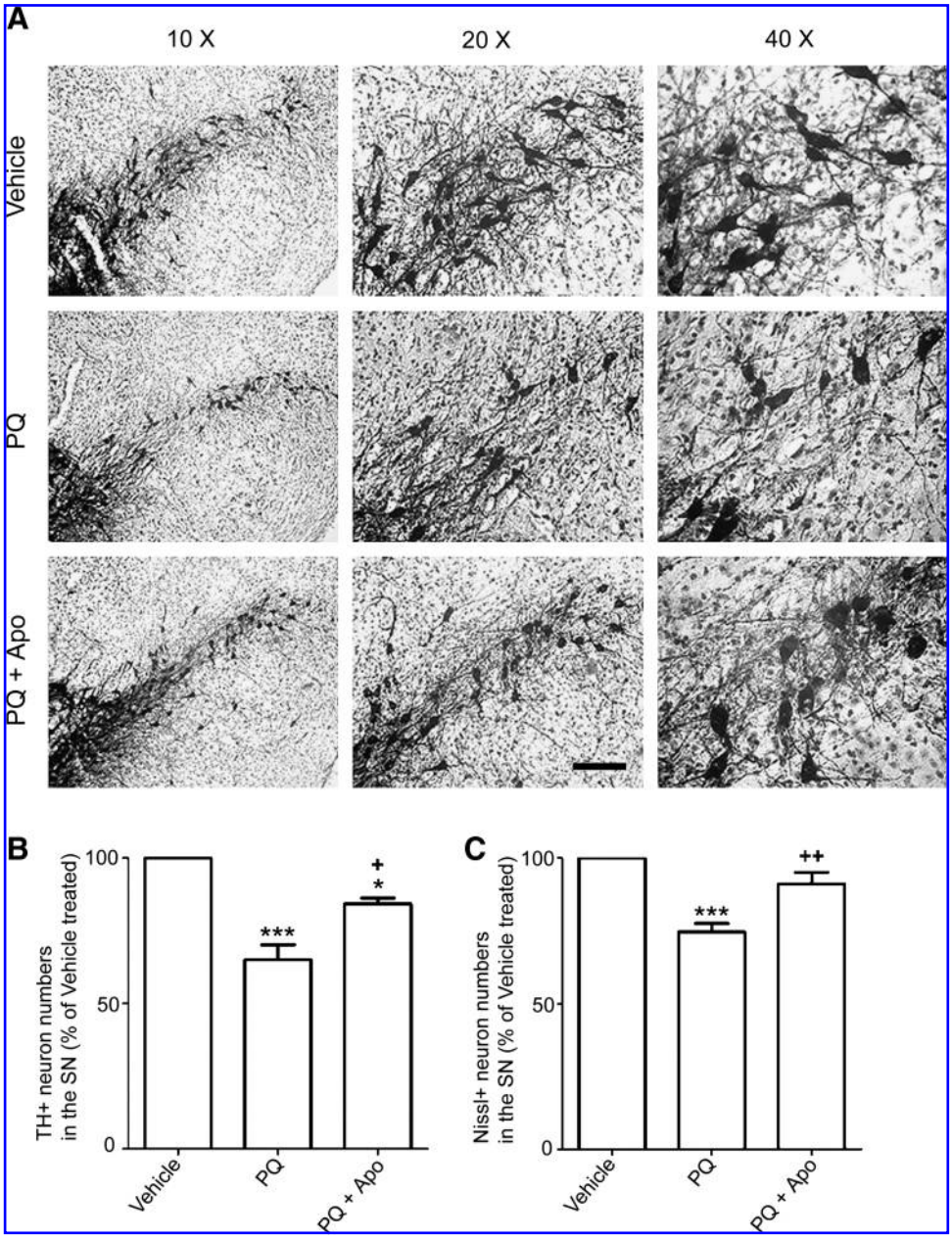

FIG. 7. Apocynin reduced SNDA neuronal death induced by PQ in a mouse PD model. (**A**) Representative photomicrographs of TH-immunostaining and Nissl counterstaining in the SNpc of mice treated with vehicle, PQ alone, or PQ and apocynin. Scale bar in the middle panel, 200 μm. (**B**) Changes in the number of TH-immunoreactive neurons in the SNpc after PQ treatment in the presence or absence of apocynin. The number of TH-positive neurons was statistically decreased in animals treated with PQ. This decrease was significantly attenuated in mice co-treated with PQ and apocynin. (**C**) Changes in the numbers of total neurons (Nissl staining) in the SNpc after PQ treatment in the presence or absence of apocynin. The number of total neurons was statistically decreased in animals treated with PQ. This decrease was significantly attenuated in mice co-treated with PQ and apocynin. The results are expressed as percentage of vehicle. Data are shown as the mean ± SEM (vehicle group, $n = 6$; PQ group, $n = 7$; Apo+ PQ group, $n = 5$). Statistical analysis was performed by using one-way ANOVA followed by Bonferroni's Multiple Comparison Test. *$p < 0.05$ and ***$p < 0.001$ *versus* mice treated with vehicle; $^{\dagger}p < 0.05$ and $^{\dagger\dagger}p < 0.01$ *versus* mice treated with PQ.

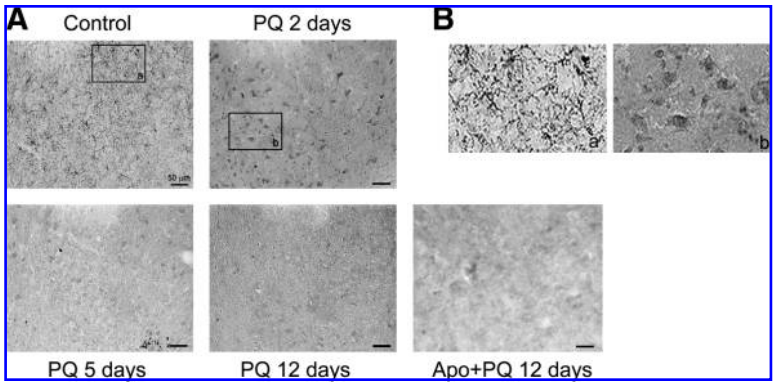

FIG. 8. The time-course decrease in CD11b-positive microglia in mice treated with PQ. (**A**) Representative photomicrographs of four independent experiments depicting CD11b-positive microglial immunostaining in the SNpc of mice treated with vehicle, PQ, or Apo+ PQ at days 2, 5, and 12. Changes are observed in the number of CD11b-immunoreactive cells in the SNpc after PQ and Apo+PQ treatment. (**B**) Higher magnification of respective boxed areas in (**A**). Control, vehicle treated; PQ 2, 5, 12 days, PQ treated; Apo+PQ 12 days, PQ and apocynin co-treatment. (Control, $n = 5$; PQ group, $n = 7$; Apo+PQ group, $n = 5$). Scale bar, 50 μm.

Microglia are another cellular component in brain parenchyma affected by PQ administration. PQ activates Nox-mediated superoxide generation in BV2 microglia (43). Primary neuron–microglia mixed culture treated with a low concentration of PQ (1 μM) showed selective DA cell death, whereas microglia-depleted cultures or neuron–microglia mixed cultures of Nox2-null mice were resistant to PQ exposure. This result suggests that DA neurotoxicity is indirectly caused by low-dose PQ-mediated microglial Nox2 activation (59). In the present study, however, a significant decrease in the number of CD11b-positive microglia was observed in PQ-treated mice, suggesting that the PQ-injection paradigm used in the present study could be highly toxic to microglia.

It is well recognized that apocynin can act as a NADPH oxidase inhibitor, and its neuroprotective effects have been reported in several CNS disorders. ALS mice treated with apocynin showed an increase in their average life spans (27). In the ketamine-induced schizophrenia animal model, inhibition of NADPH oxidase by apocynin prevents the dysfunction of cortical inhibitory interneurons elicited by ketamine and reduced NADPH oxidase activity (8). In the experimental stroke model using middle cerebral artery occlusion, apocynin significantly prevents blood–brain barrier disruption (35). Recent studies, however, raised controversy that apocynin may work as an antioxidant instead of NADPH oxidase inhibitor, especially in the vascular system. The results suggest that it may have a tissue-specific role. Based on these facts, we first tested whether apocynin may reduce PQ-mediated ROS generation and cell death. Both PQ-induced ROS and DA cell death were significantly decreased by pretreatment with apocynin. We continued to investigate whether apocynin reduces SN DA neuronal death elicited by systemic administration of PQ. DA neuronal death in the SN was significantly reduced by apocynin. It was reported that in a mouse stroke model, the lower dose of apocynin administrated IV works more effectively than the higher dose (56). It might be worth while to test several different doses of apocynin in a future study.

Next, we tested the specific role of Nox1 in the PQ-mediated ROS generation and DA cell death by siRNA-mediated Nox1 knockdown. Significant decreases in both ROS and cell death were achieved by Nox1 knockdown, suggesting that Nox1 plays a significant role in PQ-mediated oxidative stress and DA cell death. In addition to Nox1 in DA neurons, Nox2 in microglia may serve as a target for apocynin. Thus, the apocynin-mediated DA neuroprotection might be a combined outcome of microglial Nox2 and neuronal Nox1 inhibitions. To clarify the role of Nox1 in the nigrostriatal DA pathway degeneration caused by PQ, further study with Nox1-knockout mice or the *in vivo* knockdown system would be necessary.

In summary, the present study demonstrated that PQ may induce its toxic effects on DA neurons by activating the Nox system, particularly Nox1, which, in turn, generates ROS and eventually results in DA neuronal death. The study also raises the possibility that dopaminergic Nox1 may serve as a novel target for pharmacologic intervention of PD.

Acknowledgments

Ana Clara Cristóvão is the recipient of a Ph.D. fellowship (SFRH/BD/15889/2005) from the Portuguese Foundation for Science and Technology (FCT). We thank Dr. Tong H. Joh for his valuable advice during the preparation of this manuscript and Kindiya D. Geghman for her critical reading and revision of the manuscript.

Author Disclosure Statement

No competing financial interests exist.

References

1. Abramov AY, Jacobson J, Wientjes F, Hothersall J, Canevari L, and Duchen MR. Expression and modulation of an NADPH oxidase in mammalian astrocytes. *J Neurosci* 25: 9176–9184, 2005.
2. Alam ZI, Daniel SE, Lees AJ, Marsden DC, Jenner P, and Halliwell B. A generalised increase in protein carbonyls in the brain in Parkinson's but not incidental Lewy body disease. *J Neurochem* 69: 1326–1329, 1997.
3. Aldieri E, Riganti C, Polimeni M, Gazzano E, Lussiana C, Campia I, and Ghigo D. Classical inhibitors of NOX NAD(P)H oxidases are not specific. *Curr Drug Metab* 9: 686–696, 2008.
4. Anantharam V, Kaul S, Song C, Kanthasamy A, and Kanthasamy AG. Pharmacological inhibition of neuronal NADPH oxidase protects against 1-methyl-4-phenylpyridinium (MPP+)-induced oxidative stress and apoptosis in mesencephalic dopaminergic neuronal cells. *Neurotoxicology* 28: 988–997, 2007.
5. Baldereschi M, Di Carlo A, Vanni P, Ghetti A, Carbonin P, Amaducci L, and Inzitari D. Lifestyle-related risk factors for Parkinson's disease: a population-based study. *Acta Neurol Scand* 108: 239–244, 2003.
6. Barnham KJ, Masters CL, and Bush AI. Neurodegenerative diseases and oxidative stress. *Nat Rev Drug Discov* 3: 205–214, 2004.
7. Beal MF. Mitochondria, oxidative damage, and inflammation in Parkinson's disease. *Ann N Y Acad Sci* 991: 120–131, 2003.
8. Behrens MM, Ali SS, Dao DN, Lucero J, Shekhtman G, Quick KL, and Dugan LL. Ketamine-induced loss of phenotype of fast-spiking interneurons is mediated by NADPH-oxidase. *Science* 318: 1645–1647, 2007.
9. Bokoch GM and Diebold BA. Current molecular models for NADPH oxidase regulation by Rac GTPase. *Blood* 100: 2692–2696, 2002.
10. Brown TP, Rumsby PC, Capleton AC, Rushton L, and Levy LS. Pesticides and Parkinson's disease: is there a link? *Environ Health Perspect* 114: 156–164, 2006.
11. Bus JS and Gibson JE. Paraquat: model for oxidant-initiated toxicity. *Environ Health Perspect* 55: 37–46, 1984.
12. Castello PR, Drechsel DA, and Patel M. Mitochondria are a major source of paraquat-induced reactive oxygen species production in the brain. *J Biol Chem* 282: 14186–14193, 2007.
13. Cevik MO, Katsuyama M, Kanda S, Kaneko T, Iwata K, Ibi M, Matsuno K, Kakehi T, Cui W, Sasaki M, and Yabe-Nishimura C. The AP-1 site is essential for the promoter activity of NOX1/NADPH oxidase, a vascular superoxide-producing enzyme: possible involvement of the ERK1/2-JunB pathway. *Biochem Biophys Res Commun* 374: 351–355, 2008.
14. Cheng G, Cao Z, Xu X, van Meir EG, and Lambeth JD. Homologs of gp91phox: cloning and tissue expression of Nox3, Nox4, and Nox5. *Gene* 269: 131–140, 2001.
15. Cheng G, Diebold BA, Hughes Y, and Lambeth JD. Nox1-dependent reactive oxygen generation is regulated by Rac1. *J Biol Chem* 281: 17718–17726, 2006.

16. Choi SH, Lee DY, Chung ES, Hong YB, Kim SU, and Jin BK. Inhibition of thrombin-induced microglial activation and NADPH oxidase by minocycline protects dopaminergic neurons in the substantia nigra in vivo. *J Neurochem* 95: 1755–1765, 2005.
17. Cohen GM and d'Arcy Doherty M. Free radical mediated cell toxicity by redox cycling chemicals. *Br J Cancer Suppl* 8: 46–52, 1987.
18. De Deken X, Wang D, Many MC, Costagliola S, Libert F, Vassart G, Dumont JE, and Miot F. Cloning of two human thyroid cDNAs encoding new members of the NADPH oxidase family. *J Biol Chem* 275: 23227–23233, 2000.
19. Desouki MM, Kulawiec M, Bansal S, Das GM, and Singh KK. Cross talk between mitochondria and superoxide generating NADPH oxidase in breast and ovarian tumors. *Cancer Biol Ther* 4: 1367–1373, 2005.
20. Dexter DT, Carter CJ, Wells FR, Javoy-Agid F, Agid Y, Lees A, Jenner P, and Marsden CD. Basal lipid peroxidation in substantia nigra is increased in Parkinson's disease. *J Neurochem* 52: 381–389, 1989.
21. Dexter DT, Wells FR, Lees AJ, Agid F, Agid Y, Jenner P, and Marsden CD. Increased nigral iron content and alterations in other metal ions occurring in brain in Parkinson's disease. *J Neurochem* 52: 1830–1836, 1989.
22. Drechsel DA and Patel M. Role of reactive oxygen species in the neurotoxicity of environmental agents implicated in Parkinson's disease. *Free Radic Biol Med* 44: 1873–1886, 2008.
23. Fan CY, Katsuyama M, and Yabe-Nishimura C. PKCdelta mediates up-regulation of NOX1, a catalytic subunit of NADPH oxidase, via transactivation of the EGF receptor: possible involvement of PKCdelta in vascular hypertrophy. *Biochem J* 390: 761–767, 2005.
24. Gao HM, Liu B, and Hong JS. Critical role for microglial NADPH oxidase in rotenone-induced degeneration of dopaminergic neurons. *J Neurosci* 23: 6181–6187, 2003.
25. Graham DG. Oxidative pathways for catecholamines in the genesis of neuromelanin and cytotoxic quinones. *Mol Pharmacol* 14: 633–643, 1978.
26. Griffiths PD, Dobson BR, Jones GR, and Clarke DT. Iron in the basal ganglia in Parkinson's disease: an in vitro study using extended X-ray absorption fine structure and cryo-electron microscopy. *Brain* 122(Pt 4): 667–673, 1999.
27. Harraz MM, Marden JJ, Zhou W, Zhang Y, Williams A, Sharov VS, Nelson K, Luo M, Paulson H, Schoneich C, and Engelhardt JF. SOD1 mutations disrupt redox-sensitive Rac regulation of NADPH oxidase in a familial ALS model. *J Clin Invest* 118: 659–670, 2008.
28. Hertzman C, Wiens M, Bowering D, Snow B, and Calne D. Parkinson's disease: a case-control study of occupational and environmental risk factors. *Am J Ind Med* 17: 349–355, 1990.
29. Heumuller S, Wind S, Barbosa-Sicard E, Schmidt HH, Busse R, Schroder K, and Brandes RP. Apocynin is not an inhibitor of vascular NADPH oxidases but an antioxidant. *Hypertension* 51: 211–217, 2008.
30. Hunot S, Boissiere F, Faucheux B, Brugg B, Mouatt-Prigent A, Agid Y, and Hirsch EC. Nitric oxide synthase and neuronal vulnerability in Parkinson's disease. *Neuroscience* 72: 355–363, 1996.
31. Ibi M, Katsuyama M, Fan C, Iwata K, Nishinaka T, Yokoyama T, and Yabe-Nishimura C. NOX1/NADPH oxidase negatively regulates nerve growth factor-induced neurite outgrowth. *Free Radic Biol Med* 40: 1785–1795, 2006.
32. Ibi M, Matsuno K, Shiba D, Katsuyama M, Iwata K, Kakehi T, Nakagawa T, Sango K, Shirai Y, Yokoyama T, Kaneko S, Saito N, and Yabe-Nishimura C. Reactive oxygen species derived from NOX1/NADPH oxidase enhance inflammatory pain. *J Neurosci* 28: 9486–9494, 2008.
33. Infanger DW, Sharma RV, and Davisson RL. NADPH oxidases of the brain: distribution, regulation, and function. *Antioxid Redox Signal* 8: 1583–1596, 2006.
34. Jenner P. Oxidative stress in Parkinson's disease. *Ann Neurol* 53(suppl 3): S26–S36; discussion S36–S28, 2003.
35. Kahles T, Luedike P, Endres M, Galla HJ, Steinmetz H, Busse R, Neumann-Haefelin T, and Brandes RP. NADPH oxidase plays a central role in blood-brain barrier damage in experimental stroke. *Stroke* 38: 3000–3006, 2007.
36. Kim MJ, Shin KS, Chung YB, Jung KW, Cha CI, and Shin DH. Immunohistochemical study of p47phox and gp91phox distributions in rat brain. *Brain Res* 1040: 178–186, 2005.
37. Kim YS, Choi DH, Block ML, Lorenzl S, Yang L, Kim YJ, Sugama S, Cho BP, Hwang O, Browne SE, Kim SY, Hong JS, Beal MF, and Joh TH. A pivotal role of matrix metalloproteinase-3 activity in dopaminergic neuronal degeneration via microglial activation. *FASEB J* 21: 179–187, 2007.
38. Lee SB, Bae IH, Bae YS, and Um HD. Link between mitochondria and NADPH oxidase 1 isozyme for the sustained production of reactive oxygen species and cell death. *J Biol Chem* 281: 36228–36235, 2006.
39. Liou HH, Tsai MC, Chen CJ, Jeng JS, Chang YC, Chen SY, and Chen RC. Environmental risk factors and Parkinson's disease: a case-control study in Taiwan. *Neurology* 48: 1583–1588, 1997.
40. Manning-Bog AB, McCormack AL, Li J, Uversky VN, Fink AL, and Di Monte DA. The herbicide paraquat causes up-regulation and aggregation of alpha-synuclein in mice: paraquat and alpha-synuclein. *J Biol Chem* 277: 1641–1644, 2002.
41. McCormack AL, Atienza JG, Johnston LC, Andersen JK, Vu S, and Di Monte DA. Role of oxidative stress in paraquat-induced dopaminergic cell degeneration. *J Neurochem* 93: 1030–1037, 2005.
42. McCormack AL, Thiruchelvam M, Manning-Bog AB, Thiffault C, Langston JW, Cory-Slechta DA, and Di Monte DA. Environmental risk factors and Parkinson's disease: selective degeneration of nigral dopaminergic neurons caused by the herbicide paraquat. *Neurobiol Dis* 10: 119–127, 2002.
43. Miller RL, Sun GY, and Sun AY. Cytotoxicity of paraquat in microglial cells: Involvement of PKCdelta- and ERK1/2-dependent NADPH oxidase. *Brain Res* 1167: 129–139, 2007.
44. Nikolova S, Lee YS, and Kim JA. Rac1-NADPH oxidase-regulated generation of reactive oxygen species mediates glutamate-induced apoptosis in SH-SY5Y human neuroblastoma cells. *Free Radic Res* 39: 1295–1304, 2005.
45. Peng J, Stevenson FF, Doctrow SR, and Andersen JK. Superoxide dismutase/catalase mimetics are neuroprotective against selective paraquat-mediated dopaminergic neuron death in the substantial nigra: implications for Parkinson disease. *J Biol Chem* 280: 29194–29198, 2005.
46. Perry TL, Godin DV, and Hansen S. Parkinson's disease: a disorder due to nigral glutathione deficiency? *Neurosci Lett* 33: 305–310, 1982.
47. Purisai MG, McCormack AL, Cumine S, Li J, Isla MZ, and Di Monte DA. Microglial activation as a priming event leading to paraquat-induced dopaminergic cell degeneration. *Neurobiol Dis* 25: 392–400, 2007.
48. Rajagopalan S, Kurz S, Munzel T, Tarpey M, Freeman BA, Griendling KK, and Harrison DG. Angiotensin II-mediated

hypertension in the rat increases vascular superoxide production via membrane NADH/NADPH oxidase activation: contribution to alterations of vasomotor tone. *J Clin Invest* 97: 1916–1923, 1996.
49. Richardson JR, Quan Y, Sherer TB, Greenamyre JT, and Miller GW. Paraquat neurotoxicity is distinct from that of MPTP and rotenone. *Toxicol Sci* 88: 193–201, 2005.
50. Rossi F and Zatti M. Biochemical aspects of phagocytosis in polymorphonuclear leucocytes: NADH and NADPH oxidation by the granules of resting and phagocytizing cells. *Experientia* 20: 21–23, 1964.
51. Schapira AH, Cooper JM, Dexter D, Jenner P, Clark JB, and Marsden CD. Mitochondrial complex I deficiency in Parkinson's disease. *Lancet* 1: 1269, 1989.
52. Serrano F, Kolluri NS, Wientjes FB, Card JP, and Klann E. NADPH oxidase immunoreactivity in the mouse brain. *Brain Res* 988: 193–198, 2003.
53. Sherer TB, Kim JH, Betarbet R, and Greenamyre JT. Subcutaneous rotenone exposure causes highly selective dopaminergic degeneration and alpha-synuclein aggregation. *Exp Neurol* 179: 9–16, 2003.
54. Sofic E, Lange KW, Jellinger K, and Riederer P. Reduced and oxidized glutathione in the substantia nigra of patients with Parkinson's disease. *Neurosci Lett* 142: 128–130, 1992.
55. Suh YA, Arnold RS, Lassegue B, Shi J, Xu X, Sorescu D, Chung AB, Griendling KK, and Lambeth JD. Cell transformation by the superoxide-generating oxidase Mox1. *Nature* 401: 79–82, 1999.
56. Tang XN, Cairns B, Cairns N, and Yenari MA. Apocynin improves outcome in experimental stroke with a narrow dose range. *Neuroscience* 154: 556–562, 2008.
57. Tejada-Simon MV, Serrano F, Villasana LE, Kanterewicz BI, Wu GY, Quinn MT, and Klann E. Synaptic localization of a functional NADPH oxidase in the mouse hippocampus. *Mol Cell Neurosci* 29: 97–106, 2005.
58. Ueyama T, Geiszt M, and Leto TL. Involvement of Rac1 in activation of multicomponent Nox1- and Nox3-based NADPH oxidases. *Mol Cell Biol* 26: 2160–2174, 2006.
59. Wu XF, Block ML, Zhang W, Qin L, Wilson B, Zhang WQ, Veronesi B, and Hong JS. The role of microglia in paraquat-induced dopaminergic neurotoxicity. *Antioxid Redox Signal* 7: 654–661, 2005.
60. Zhang J, Perry G, Smith MA, Robertson D, Olson SJ, Graham DG, and Montine TJ. Parkinson's disease is associated with oxidative damage to cytoplasmic DNA and RNA in substantia nigra neurons. *Am J Pathol* 154: 1423–1429, 1999.

Address correspondence to:
Dr. Yoon-Seong Kim, M.D., Ph.D.
Weill Medical College of Cornell University
Neurology/Neuroscience, A578
525 East 68th Street
New York, New York 10065

E-mail: yok2001@med.cornell.edu

Date of first submission to ARS Central, January 16, 2009; date of final revised submission, May 14, 2009; date of acceptance, May 17, 2009.

Abbreviations Used

Apo = apocynin
CNS = central nervous system
DA = dopaminergic
DCFDA = 2′,7′-dichlorodihydrofluorescein diacetate
DHE = dihydroethidium
DMSO = dimethyl sulfoxide
FCCP = carbonylcyanide-4-(trifluoromethoxy)-phenylhydrazo
GAPDH = glyceraldehyde 3-phosphate dehydrogenase
IP = intraperitoneal
LDH = lactate dehydrogenase
MPP^+ = 1-methyl-4-phenylpyridinium
MPTP = 1-methyl-4-phenyl-1,2,3,6-tetrahydropyridine
MTT = 3-(4,5-dimethylthiazal-2-yl)-2,5-diphenyl-tetrazolium bromide
NADPH = nicotinamide adenine dinucleotide phosphate
NBT = nitroblue tetrazolium
NO = nitrogen oxide
Nox = NADPH oxidase
Nox1 = NADPH oxidase 1
Nox2 = $gp91^{phox}$
Nox3 = NADPH oxidase 3
Nox4 = NADPH oxidase 4 OH^-, hydroxyl radical
PD = Parkinson's disease
PQ = paraquat
ROS = reactive oxygen species
SN = substantia nigra
SNpc = SN pars compacta
TH = tyrosine hydroxylase

This article has been cited by:

1. Grace Y. Sun, Yan He, Dennis Y. Chuang, James C. Lee, Zezong Gu, Agnes Simonyi, Albert Y. Sun. 2012. Integrating Cytosolic Phospholipase A2 with Oxidative/Nitrosative Signaling Pathways in Neurons: A Novel Therapeutic Strategy for AD. *Molecular Neurobiology* **46**:1, 85-95. [CrossRef]
2. Hee-Seong Jang, Jee In Kim, Jinu Kim, Yeon Kyung Na, Jeen-Woo Park, Kwon Moo Park. 2012. Bone marrow derived cells and reactive oxygen species in hypertrophy of contralateral kidney of transient unilateral renal ischemia-induced mouse. *Free Radical Research* **46**:7, 903-911. [CrossRef]
3. Silvia Sorce, Karl-Heinz Krause, Vincent Jaquet. 2012. Targeting NOX enzymes in the central nervous system: therapeutic opportunities. *Cellular and Molecular Life Sciences* **69**:14, 2387-2407. [CrossRef]
4. Leonard P. Rybak, Debashree Mukherjea, Sarvesh Jajoo, Tejbeer Kaur, Vickram Ramkumar. 2012. siRNA-mediated knock-down of NOX3: therapy for hearing loss?. *Cellular and Molecular Life Sciences* **69**:14, 2429-2434. [CrossRef]
5. Sudipta Chakraborty, Michael Aschner. 2012. Altered manganese homeostasis: Implications for BLI-3-dependent dopaminergic neurodegeneration and SKN-1 protection in C. elegans. *Journal of Trace Elements in Medicine and Biology* **26**:2-3, 183-187. [CrossRef]
6. Dong-Hee Choi , Ana Clara Cristóvão , Subhrangshu Guhathakurta , Jongmin Lee , Tong H. Joh , M. Flint Beal , Yoon-Seong Kim . 2012. NADPH Oxidase 1-Mediated Oxidative Stress Leads to Dopamine Neuron Death in Parkinson's Disease. *Antioxidants & Redox Signaling* **16**:10, 1033-1045. [Abstract] [Full Text HTML] [Full Text PDF] [Full Text PDF with Links] [Supplemental material]
7. Aracely Garcia-Garcia , Laura Zavala-Flores , Humberto Rodriguez-Rocha , Rodrigo Franco . Thiol-Redox Signaling, Dopaminergic Cell Death, and Parkinson's Disease. *Antioxidants & Redox Signaling*, ahead of print. [Abstract] [Full Text HTML] [Full Text PDF] [Full Text PDF with Links]
8. Hui-Ming Gao, Hui Zhou, Jau-Shyong Hong. 2012. NADPH oxidases: novel therapeutic targets for neurodegenerative diseases. *Trends in Pharmacological Sciences* . [CrossRef]
9. Khanh vinh quôc Luong, Lan Thi Hoàng Nguyên. 2012. Vitamin D and Parkinson's disease. *Journal of Neuroscience Research* n/a-n/a. [CrossRef]
10. P. M. Rappold, M. Cui, A. S. Chesser, J. Tibbett, J. C. Grima, L. Duan, N. Sen, J. A. Javitch, K. Tieu. 2011. Paraquat neurotoxicity is mediated by the dopamine transporter and organic cation transporter-3. *Proceedings of the National Academy of Sciences* . [CrossRef]
11. Ashutosh Kumar, Brajesh Kumar Singh, Israr Ahmad, Smriti Shukla, Devendra Kumar Patel, Garima Srivastava, Vinod Kumar, Haushila Prasad Pandey, Chetna Singh. 2011. Involvement of NADPH oxidase and glutathione in zinc-induced dopaminergic neurodegeneration in rats: Similarity with paraquat neurotoxicity. *Brain Research* . [CrossRef]
12. Rita Martins, João António Queiroz, Fani Sousa. 2011. Histidine affinity chromatography-based methodology for the simultaneous isolation of Escherichia coli small and ribosomal RNA. *Biomedical Chromatography* n/a-n/a. [CrossRef]
13. Qing Li, Xiujuan Peng, Hyekyung Yang, Hongbing Wang, Yan Shu. 2011. Deficiency of Multidrug and Toxin Extrusion 1 Enhances Renal Accumulation of Paraquat and Deteriorates Kidney Injury in Mice. *Molecular Pharmaceutics* 111012113144003. [CrossRef]
14. Brajesh Kumar Singh, Ashutosh Kumar, Israr Ahmad, Vinod Kumar, Devendra Kumar Patel, Swatantra Kumar Jain, Chetna Singh. 2011. Oxidative stress in zinc-induced dopaminergic neurodegeneration: Implications of superoxide dismutase and heme oxygenase-1. *Free Radical Research* **45**:10, 1207-1222. [CrossRef]
15. David Cantu, Ruth E. Fulton, Derek A. Drechsel, Manisha Patel. 2011. Mitochondrial aconitase knockdown attenuates paraquat-induced dopaminergic cell death via decreased cellular metabolism and release of iron and H2O2. *Journal of Neurochemistry* **118**:1, 79-92. [CrossRef]
16. Lijing Liu, Feng Cui, Qingliang Li, Bojiao Yin, Huawei Zhang, Baoying Lin, Yaorong Wu, Ran Xia, Sanyuan Tang, Qi Xie. 2011. The endoplasmic reticulum-associated degradation is necessary for plant salt tolerance. *Cell Research* **21**:6, 957-969. [CrossRef]
17. Kyeong Ah Kim, Ju Young Kim, Young Ah Lee, Kyoung-Ju Song, Deulle Min, Myeong Heon Shin. 2011. NOX1 participates in ROS-dependent cell death of colon epithelial Caco2 cells induced by Entamoeba histolytica. *Microbes and Infection* . [CrossRef]
18. Albert Sun, Qun Wang, Agnes Simonyi, Grace SunBotanical Phenolics and Neurodegeneration **20115386**, 315-332. [CrossRef]

19. Katie Facecchia, Lee-Anne Fochesato, Sidhartha D. Ray, Sidney J. Stohs, Siyaram Pandey. 2011. Oxidative Toxicity in Neurodegenerative Diseases: Role of Mitochondrial Dysfunction and Therapeutic Strategies. *Journal of Toxicology* **2011**, 1-12. [CrossRef]
20. W Michael Zawada, Gregg P Banninger, Jennifer Thornton, Beth Marriott, David Cantu, Angela L Rachubinski, Mita Das, W Sue T Griffin, Susan M Jones. 2011. Generation of reactive oxygen species in 1-methyl-4-phenylpyridinium (MPP+) treated dopaminergic neurons occurs as an NADPH oxidase-dependent two-wave cascade. *Journal of Neuroinflammation* **8**:1, 129. [CrossRef]
21. We Ge, Yingmei Zhang, Xuefeng Han, Jun Ren. 2010. Cardiac-specific overexpression of catalase attenuates paraquat-induced myocardial geometric and contractile alteration: Role of ER stress. *Free Radical Biology and Medicine* **49**:12, 2068-2077. [CrossRef]
22. Rodrigo Franco, Sumin Li, Humberto Rodriguez-Rocha, Michaela Burns, Mihalis I. Panayiotidis. 2010. Molecular mechanisms of pesticide-induced neurotoxicity: Relevance to Parkinson's disease. *Chemico-Biological Interactions* **188**:2, 289-300. [CrossRef]
23. Gayle Gordillo , Huiqing Fang , Hana Park , Sashwati Roy . 2010. Nox-4–Dependent Nuclear H2O2 Drives DNA Oxidation Resulting in 8-OHdG as Urinary Biomarker and Hemangioendothelioma Formation. *Antioxidants & Redox Signaling* **12**:8, 933-943. [Abstract] [Full Text HTML] [Full Text PDF] [Full Text PDF with Links] [Supplemental material]
24. Bobby Thomas . 2009. Parkinson's Disease: From Molecular Pathways in Disease to Therapeutic Approaches. *Antioxidants & Redox Signaling* **11**:9, 2077-2082. [Abstract] [Full Text HTML] [Full Text PDF] [Full Text PDF with Links]